

### 4D.3 The Double Eyewall and Cycloid-like Track in the Typhoon Dujuan (2003)

Jing-Shan Hong, and P.-L. Chang  
 Central Weather Bureau, Taipei, Taiwan

#### 1. INTRODUCTION

The trochoidal motions are often found in double eyewall cases in typhoons or hurricanes (Jordan 1966, Muramatsu 1986). Typhoon Dujuan (2003) formed in the West Pacific Ocean at 1200 UTC 29 Aug, 2003; the storm then began a northward moving, passed to the south of Taiwan at 1535 UTC 1 Sep, and made a direct hit on Hongkong at about 1200 UTC 2 September. As Dujuan neared Taiwan, the prominent double eyewall was observed as the storm moved within the range of the RCKT Doppler radar. Typhoon Dujuan had an unusual feature that the inner eye orbited in the moat with period of 3.5–4 h and eventually exhibited as a cycloid-like track. Thus, the oscillated track pattern and the associated eyewall structures in radar view are further analyzed and given in the paper.

#### 2. RESULT

Fig. 1 is the snapshot of the composite radar reflectivity field at 1159 UTC 1 Sep 2003 and showed a distinct double eyewall in the center of typhoon Dujuan. As shown in Fig. 1, the inner eyewall was associated with strong reflectivity up to 55 dBz within radial scale of about 10 km. The outer ring was characterized as broader convective zone around south of Taiwan and the stripped spiral convective bands over east and north of typhoon. Of particular importance is that the double eyewall in typhoon Dujuan was not concentric. Thus the inner eye tended to circulate due to the steering of the rotational flow in

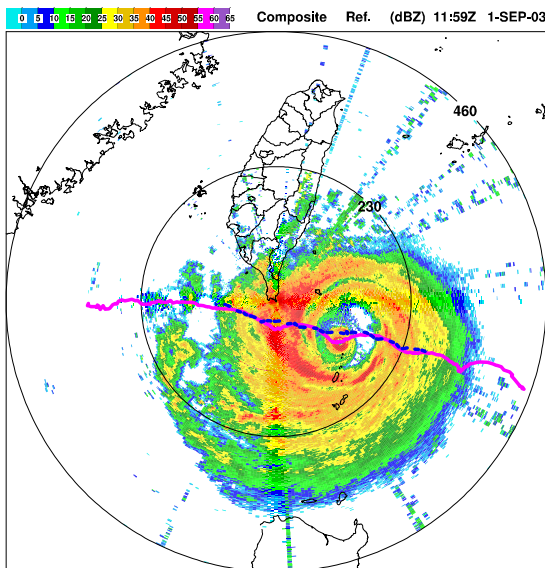


Fig. 1. The snapshot of the composite radar reflectivity field of 0.5° PPI at 1159 UTC 1 Sep 2003. The track of the outer ring and inner eye derived from the 8-min Doppler radar scans are represented by the dash and solid line. Range rings extend concentrically outward at 230-km intervals from the RCKT.

the moat. The orbited inner eye superimposed the mean typhoon motion therefore resulted in a cycloid-like track pattern of the inner eye. In Dujuan, total of four obviously cycloid-like arches were identified within the range of the radar observations before the typhoon passed over south of Taiwan. Each arch from east to west had the period of 3-h 52-min, 3-h 44-min, 3-h 36-min, and 3-h 20-min, respectively. The period of the arch was slightly decreased as typhoon approaching Taiwan Island. As Dujuan moved closer to the RCKT, reflectivity field at the 0.5° PPI for two complete cycloid-like arches sampled in 40-min intervals were further analyzed.

The RMW associated with the outer ring was continuously contracted from about 120 km to 45 km (Fig. 2) while the RMW associated with the inner eye was about 20 km and almost kept constant. Fig. 2 exhibited the details of the contraction process and exhibited as two phases, roughly separated from each arch. The first phase was contracted from 120 to 68 km and associated with an obviously spin-up of the tangential wind from 48 to 60 m s<sup>-1</sup> in 4 hours. The contraction and spin-up, in particular for the outbound radial velocities, were most significant between 1040~1224 UTC, which was coincidence with the active convection occurred between the typhoon and Taiwan topography (not shown here). Thus, Taiwan topography is suggested to enhance the convection as the storm was approaching and then resulted in the spin-up and contraction.

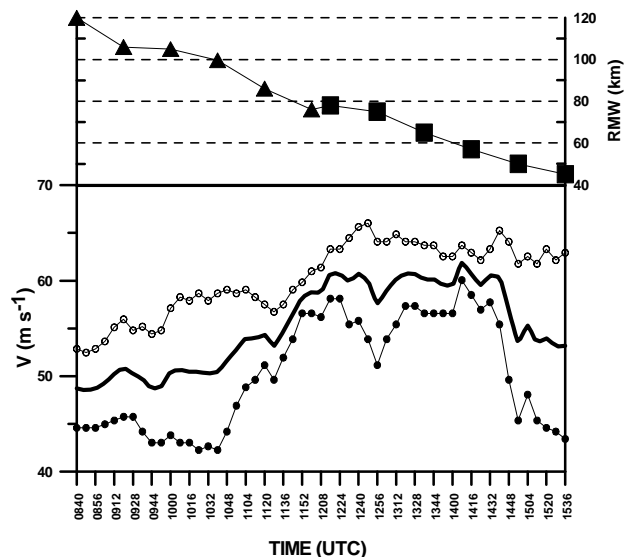


Fig. 2. Time series plot of RMW (above), the triangles and squares are corresponding to the RMW in the two arches. Below are the maximum inbound (hollow circles)/outbound (solid circles) radial velocities of the outer ring. The heavy line is the mean of the maximum inbound/outbound velocity.

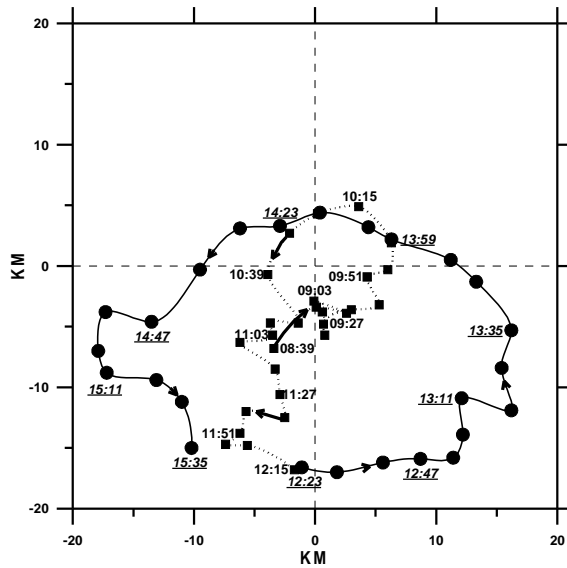


Fig. 3. The orbit of the centers of the inner eye relative to the outer ring. The center of the outer ring is fixed at coordinate of (0, 0). Dashed and Solid lines indicate the orbit of the inner eye in the arches displayed in Fig. 3 and 4, respectively. The numbers in *arial* and *Italics* are the time stamp in every 24 min for the two arches. The arrays indicate the direction of the orbit.

The RMW of the outer ring tended to contract *linearly* from 78 to 45 km in the second phase. However, the tangential wind almost kept constant in the beginning of the phase and then spin-down abruptly (especially for the out bound radial velocity) at 1432 UTC. Topography again is suggested to play the role to directly spin down the tangential wind as the storm neared Taiwan and then increase the inward flow component due to the unbalanced pressure gradient force. This increased inward flow further resulted in the contraction of the outer ring and the enhanced convection as storm closed to the topography (not shown).

Fig. 3 depicted the orbit of the inner eye relative to the center of the outer ring for the aforementioned two complete cycloid-like arches. The figure showed that the cyclonic oscillation with amplitude about 10-km in the first arch started from 0839 UTC and tended to be rather symmetric to the center of the outer ring. The inner eyes then moved to further south during the end of the arch and started to the beginning of the second arch. However, the amplitude of the second arch was larger than the first one and up to 30 km in the east-west and 20 km in the south-north. The orbit of the inner eye was roughly symmetry in the east-west and obviously shifted to the south portion. The vertical wind shear derived from the composite dropsonde showed a significant northerly vertical shear from 700 to 300 hPa ( $15 \text{ m s}^{-1}/400 \text{ hPa}$ ). On the other hand, the vertical development of the inner eyewall was up to 10~12 km whereas only 7 km for the outer ring (not shown). Thus, the inner eye was suggested to experience more forcing of the vertical wind shear than the outer ring and tended to drift to the south portion of the moat.

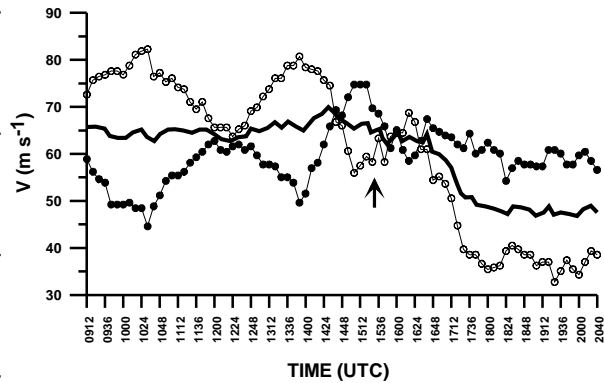


Fig. 4. Time series plot of the maximum inbound (hollow circles), outbound (solid circles) radial velocities, and the mean of the maximum inbound and outbound radial velocity of the inner eyewall from 0944 to 2138 UTC. The array indicates the time typhoon Dujan passed over RCKT radar center.

Orbited inner eye also contributed to the oscillation of the observed maximum inbound/outbound velocity as shown in Fig. 4. Apparently, the motion of the outer ring and the orbited inner eye projected to the radial component and resulted in the oscillation of the observed inbound and outbound radial velocity. The impact of the oscillation appeared in two folds. First, the projection of the motion of the outer ring and the orbited inner eye could produce a wind burst up to  $15 \text{ m s}^{-1}$  on the inbound/outbound velocity in certain condition depending on the relative relation of typhoon motion and the orbit of the inner eye. Second, the oscillation of the inbound/outbound velocity associated with the inner eye can enhance the wind shear across the moat. For example, the difference of the inbound velocity between the inner eye and outer ring was up to  $24 \text{ m s}^{-1}$  at 1032 UTC (Fig. 2 and 4). The large differences could enhance the differential rotation in the moat region and result in the inactive inner eye and the spiral band wrapped around the outer ring as the type 1 instability proposed by Kossin et al. (2002).

### 3. ACKNOWLEDGMENTS

This research was supported by the National Science Council of Taiwan under Grant NSC 92-2119-M-052 -002-AP1 and NSC 92-2111-M-052 -002-AP2.

### 4. REFERENCE

- Jordan, C. L., 1966: Surface pressure variations at coastal stations during the period of irregular motion of Hurricane Carla of 1961. *Mon. Wea. Rev.*, **94**, 454 – 458.
- Kossin, J. P., Schubert, W. H., Montgomery, M. T., 2000: Unstable Interactions between a Hurricane's Primary Eyewall and a Secondary Ring of Enhanced Vorticity. *J. Atmos. Sci.*, **57**, 3893 – 3917.
- Muramatsu, T., 1986: Trochoidal motion of the eye of Typhoon 8019. *J. Meteor. Soc. Japan*, **64**, 259-272.